J|A|C|S
ARTICLES

Published on Web 04/20/2010

Ethoxycarbonyl-Based Organic Electrode for Li-Batteries

Wesley Walker,[†,‡] Sylvie Grugeon,[†] Olivier Mentre,[§] Stéphane Laruelle,[†] Jean-Marie Tarascon,*[,†,‡] and Fred Wudl[‡]

LRCS, UMR 6007, Université de Picardie Jules Verne, 80039 Amiens, France, Materials Department, University of California, Santa Barbara, California 93106, and UCCS, CNRS UMR 8181, ENSCL-UST Lille 1, BP 90108, 59652 Villeneuve d'Ascq cédex, France

Received February 12, 2010; E-mail: jean-marie.tarascon@sc.u-picardie.fr

Abstract: Currently, batteries are being both considered and utilized in a variety of large-scale applications. Materials sustainability stands as a key issue for future generations of batteries. One alternative to the use of a finite supply of mined materials is the use of renewable organic materials. However, before addressing issues regarding the sustainability of a given organic electrode, fundamental questions relating to the structure−function relationships between organic components and battery performance must first be explored. Herein we report the synthesis, characterization, and device performance of an organic salt, lithium 2,6-bis(ethoxycarbonyl)-3,7-dioxo-3,7-dihydro-*s*-indacene-1,5-bis(olate), capable of reversibly intercalating with minimal polarization 1.8 Li per unit formula over two main voltage plateaus located at ∼1.96 and ∼1.67 V (vs. Li/Li$^+$), leading to an overall capacity of 125 mAh/g. Proton NMR and in situ XRD analyses of battery cycling versus Li at room temperature reveal that the insertion−deinsertion process is fully reversible with the dips in the voltage−composition traces, which are associated with changes in the 3D structural packing of the electrochemically active molecules.

Introduction

Rechargeable Li-ion batteries dominate the portable electronics market because Li-ion cells offer the largest energy density and output voltage of all the rechargeable battery technologies available. Additionally, they are well-positioned to take over the emerging large-scale application markets of electric vehicles and off-grid storage devices. In current commercial Li-ion batteries, the electrode materials are largely procured through the mining of a finite material; in addition, obtaining these materials for batteries is both energetically demanding and generates a significant amount of carbon emissions. This problem is further exacerbated by the fact that the electrode materials are commonly manufactured by energetically demanding ceramic processes. Therefore, it is advisible, owing to the ever-increasing importance of Li-ion technology, to consider all aspects of the manufacturing life cycle (i.e., scarcity of materials, carbon foot print, etc.) when designing the next generation of Li-ion batteries.[1,2]

Fortunately, the chemistry behind Li-ion technology is such that a wide range of materials can potentially be utilized. Organic molecules are intriguing candidates for electrode materials because organic synthetic techniques allow for a large amount of control over structure and functional groups, and these organic compounds are potentially renewable as many can be synthesized from natural products and biomass. Early attempts to incorporate organic molecules into batteries have revolved around conjugated polymers;[3−5] however, electrodes manufactured from conducting polymers tend to have low specific energies, are expensive to manufacture, and experience batch-to-batch variations. Recently, our research group has focused on organic molecules containing carbonyl functional groups and has found candidates for both high and low redox materials.[6−9] Through our efforts, we have gained a certain amount of control over redox potentials by utilizing more or less electron-withdrawing carbonyl groups; however, a complete understanding of the structure−function relationship of these compounds currently remains elusive, as a survey of organic compounds has resulted in few secondary battery candidates and an incomplete understanding of what structural elements lead to higher lithium loadings, degree of polarization, and electrode durability. The characterization of lithium 2,6-bis(ethoxycarbonyl)-3,7-dioxo-3,7-dihydro-*s*-indacene-1,5-bis(olate) as an electrode material helps to further define the structure/function relationship between organic molecules and their corresponding device characteristics. However, these lessons will need to be applied to an organic system that is sustainable (i.e., from biomass) in order to realize the full potential of organic electrodes in secondary battery technology.

[†] Université de Picardie Jules Verne.
[‡] University of California, Santa Barbara.
[§] ENSCL-UST Lille 1.

(1) Tarascon, J. M.; Armand, M. *Nature* **2001**, *414*, 359.
(2) Armand, M.; Tarascon, J. M. *Nature* **2008**, *414*, 359.
(3) Novák, P.; Müller, K.; Santhanam, S. V.; Hass, O. *Chem. Rev.* **1997**, *97*, 207–281.
(4) MacDiarmid, A. G.; Yang, L. S.; Huang, W. S.; Humphrey, B. D. *Synth. Met.* **1987**, *18*, 393–398.
(5) Qu, J.; Katsumata, T.; Satoh; Wada, J.; Igarashi, J.; Mizoguchi, K.; Masuda, T. *Chem.−Eur. J.* **2007**, *13*, 7965–7973.
(6) Chen, H.; Armand, M.; Demailly, G.; Dolhem, F.; Poizot, P.; Tarascon, J. M. *ChemSusChem.* **2008**, *4*, 348.
(7) Armand, M.; Michot, C.; Ravet, N. PCT Int. Appl. 37, 1999.
(8) Chen, H.; Armand, M.; Courty, M.; Jiang, M.; Grey, C.; Dolhem, F.; Tarascon, J. M.; Poizot, P. *J. Am. Chem. Soc.* **2009**, *131*, 8984–8988.
(9) Armand, M.; Grugeon, S.; Vezin, H.; Laruelle, S.; Ribiere, P.; Poizot, P.; Tarascon, J.-M. *Nat. Mater.* **2009**, *8*, 120.

Scheme 1. Synthesis of Lithium 2,6-Bis(ethoxycarbonyl)-3,7-dioxo-3,7-dihydro-*s*-indacene-1,5-bis(olate) **4**

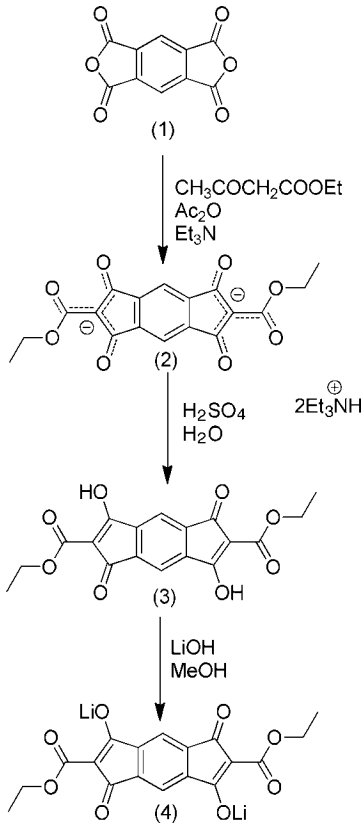

Results and Discussion

Synthesis: The synthesis of diethyl-3,7-dihydroxy-1,5-dioxo-1,5-dihydro-*s*-indacene-2,6-dicarboxylate (compound **3**, Scheme 1) was adapted from a procedure by Krief et al.[12] Synthesis began with a condensation reaction between pyromellitic anhydride (**1**) and ethyl acetoacetate in a solution of triethylamine and acetic anhydride, resulting in a black solution of the bis(triethylammonium) salt (**2**). At this point, the reaction mixture was concentrated, redissolved in water, and gravity filtered through charcoal in order to obtain a red solution. This purification departs from the original synthesis, which calls for precipitation of crystals of the bis(triethylammonium) salt at 0 °C from the reaction mixture because the original procedure resulted in poor yields and impure products. The red solution of the bis(triethylammonium) salt **2** was then acidified with sulfuric acid and filtered, resulting in the diester **3** as an orange-red powder. Compound **3** was then suspended in methanol and treated with lithium hydroxide to afford the pure dilithium salt **4**.

Single-Crystal X-ray Analysis: The recovered dilithium reddish powder was checked for its crystalline nature by X-ray diffraction. The collected diffractogram (Figure 1a) displays several intense and well-defined Bragg peaks; therefore, we could not successfully refine this experimental XRD pattern owing to the tendency of these powders to preferentially orient, most likely to optimize $\pi-\pi$ staking. To circumvent this difficulty, we went through the exercise of growing crystals. Single crystals were obtained by dissolving compound **4** in a minimal amount of boiling water, followed by slow cooling of the solution over a period of 3 h to room temperature in an oven preheated to 80 °C. The structure of the (tetrahydrated) dilithium salt **4** crystals was determined by single-crystal X-ray analysis. After selection of a suitable single crystal and subsequent data collection, the X-ray analysis confirms the molecular structure of compound **4**, with excellent final reliability factors: $R1 = 3.19\%$, $wR2 = 2.98\%$. The pertinent crystal data and characteristics of data collection and refinement are listed in Table 1. The direct methods implemented in SHELXS[10] and JANA 2000[11] were used for the structure solution and refinement, respectively. All hydrogen atoms, including those of water molecules, were located using Fourier difference maps. In the last cycles of the refinement, thermal parameters were restrained as equal for all organic protons and all water protons. The atomic and thermal parameters are given in the Supporting Information, Tables S1 and S2. Figure 2a shows an individual $Li_2C_{18}O_8H_{12}\cdot 4H_2O$ group with the corresponding label scheme and refined intramolecular distances. The H bonds and Li coordination are listed in Table 2. The tetrahydrated dilithium salt compound **4** is planar, with the cyclopentadieneone groups on each side of the molecule pointing in opposite directions. The organic molecule has two bidentate functional groups, each bridging one Li^+ by the carbonyl of the ester and the oxygen that was deprotonated with LiOH. This coordination serves to hold the ester groups in-plane (or in conjugation) with the conjugated core of the molecule. The tetrahedral coordination of lithium is achieved by two water molecules, Ow1 and Ow2, out of the molecular plane. On a macroscopic scale, the molecules orient parallel to the (121) plane in a staggered pattern, crossing at clusters of water molecules coordinated by lithium. The estimated distance between staggered layers is ~1.85 Å (Figure 2b). For reasons of completeness, we should emphasize that the XRD powder pattern of the hydrated crystals differs significantly from the diffraction pattern of the as-prepared powder of compound **4** (Figure 1a,b). It is clear that, with respect to conservation of the tetrahedral coordination of Li-cations observed in the hydrated forms, the dehydration would involve a drastic reorganization of the molecules. This leads to the assumption that, in addition to the two O2−O3 bridges, each molecule should have two additional bidentate functional groups defined by O1 and O4. Here one could easily imagine two perpendicular orientations, a and b, of the organic planes necessary to achieve tetrahedral coordination of Li-cations by O2a, O3a, O1b, and O4b within a tridimensional crystal structure. At the moment, the quality of the XRD data

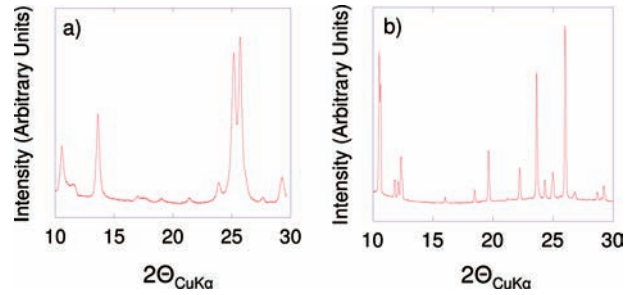

Figure 1. X-ray diffraction patterns (XRD) of (a) compound **4** as synthesized from methanol, and (b) crystals of compound **4** formed by recrystallization from water.

(10) Sheldrick, G. M. *SHELXTL*, version 5.1; Bruker AXS: Madison, WI, 1998.
(11) Petricek, V. Dusek, M. Palatinus, L. *Jana 2000*; Institute of Physics: Praha, Czech Repubic, 1997 (available from http://www-xray.fzu.cz/jana/jana.html).

Table 1. Crystal Data, Data Collection, and Structure Refinement Parameters for $Li_2C_{18}O_8H_{12}\cdot 4H_2O$

crystal data	
crystal symmetry	triclinic
space group	$P\bar{1}$
unit cell (Å and deg)	$a = 7.5387(6)$; $\alpha = 64.967(4)$ $b = 8.0616(8)$; $\beta = 83.532(4)$ $c = 9.2158(9)$; $\gamma = 81.588(4)$
volume (Å^3)	501.20(8)
Z	1
M_w, calculated density (g/cm^3)	442.2, 1.4647
$F(000)$	230

data collection	
equipment	Bruker X8
radiation Mo Kα (Å)	0.71073
scan mode	ω/φ-scan
recorded angular range θ (deg)	2.44−26.81
recording reciprocal space	$-9 \le h \le 9$ $-10 \le k \le 10$ $-11 \le l \le 1$
number of measured reflections	26045
number of independent reflections	2132
number of independent reflections [$I > 5\sigma(I)$]	1668
μ (cm^{-1}) (λ = Mo Kα)	0.123
absorption correction	multiscan (Sadabs)
transmission T_{min}/T_{max}	0.93
R merging factor (%)	3.34

refinement parameters	
software, refinement type	Jana 2000, L.S. on F
number of refined parameters	178
R_1 (F) all, [$I > 5\sigma(I)$] = $\sum\|\|F_o\| - \|F_c\|\|/\sum\|F_o\|$ (%)	3.19, 4.01
wR_2 (F^2) all, [$I > 5\sigma(I)$] = $[\sum w(F_o^2 - F_c^2)^2/\sum w(F_o^2)]^{1/2}$ (%)	2.98, 3.38
goodness of fit	0.83
weight	unit
isotropic secondary extinction	Lorentzian, 0.083425
max/min $\Delta\rho$ e/Å^3	0.22/−0.15

for anhydrous compound **4** appears insufficient to view an *ab initio* structural investigation from powder.

Electrochemical Performances. The electrochemical performance of our material was tested versus Li in a Swagelok-type cell after grinding with a mortar and pestle along with 40% carbon black (SP); it is worth noting that when samples were ball-milled for 15 min battery cycling was not reversible (not shown here) and the structure was destroyed (as deduced by XRD). Figure 3a shows the voltage−composition trace for $Li_{2+x}C_{18}H_{12}O_8$/Li cells cycled at a rate of one Li per 20 h between 3 and 0.5 V. The potential sharply drops to four separate plateaus located at ∼1.9, 1.7, 0.9, and 0.7 V before slowly tapering off to 0.5 V. Bearing in mind that the molecule contains four C═O groups, we can ascribe the plateaus at ∼1.9 and 1.7 V, whose combined amplitude is near 2 electrons, as the result of the reduction of two of the C═O groups. The pseudo-plateau near 0.9 V is reminiscent of the insertion of Li in carbon as commonly observed in negative electrodes containing carbon SP as an additive. The last pseudo-plateau at 0.7 V, whose amplitude exceeds two electrons, is the result of two reduction processes occurring simultaneously, that is, the reduction of the two remaining C═O groups per molecules which superimposes to the remaining lithiation of the carbon additive. Justification for the assignment of the last two plateaus can be found in the Supporting Information, in which a blank of the carbon additive (S5) compares well with the plateau at 0.9 V and in situ XRD experiments show no change in powder diffraction pattern across the plateau at 0.9 V, but the material becomes amorphous when cycled past the plateau at 0.7 V (S6). Unfortunately, upon charging, it is revealed that the process is irreversible, indicating that lithium uptake to 0.5 V deforms the structure of the molecule to such an extent as to make lithium-ion recovery unattainable. However, as demonstrated in Figure 3b, when $Li_{2+x}C_{18}H_{12}O_8$/Li cells were cycled at a rate of one Li per 20 h between 1.5 and 3 V, reversible cycling was noted. The potential quickly drops to reach two major plateaus; the first plateau at 1.96 V has an overall uptake capacity of 0.8 Li per unit formula, and the second plateau at 1.67 V has an overall uptake capacity of 1.0 Li per unit formula, leading to a total reversible capacity of 1.8 Li per unit formula (e.g., 125 mAh/g). This ability of the molecule to reversibly intercalate Li-ions at two discrete potentials likely results from all C═O groups on the molecule being held in conjugation with the core of the molecule by Li coordination. As one side of the molecule is reduced at 1.96 V, a subsequent charging is experienced throughout the molecule; consequently, the intercalation of a second Li into the molecule becomes more difficult, resulting in a second plateau at a lower potential (1.67 V). Each major plateau experiences a dip in potential; these dips are located at 1.90 and 1.63 V and coincide with structural changes as will be discussed later with in situ XRD data. Upon the subsequent charging cycle, the charge voltage traces the discharge voltage with minimal polarization (50−80 mV for the plateau beginning at 1.96 V, and 30−40 mV for the plateau beginning at 1.67 V) and moreover repeats all of the discharge features (e.g., voltage hints) similar to model inorganic intercalation compounds. This reversibility is further highlighted by plotting the derivative curves (dV/dQ), which show sharp redox peaks that superimpose nicely upon cycling (Figure 3b, inset). Beginning with the second cycle, an irreversible capacity of 10% is noted, and the second plateau drops to 0.8 Li uptake, while the lithium uptake of the first plateau is largely unchanged.

Additionally, a Swagelok-type cell was used to determine the electrode rate capability via the collection of a signature curve. The cell was successively discharged at decreasing rates (5C, 2.5C, 1C, 0.5C, C/4, C/10, C/20, and C/40) with a relaxation time of 30 min between each step. Inset is the classical response in potential of the newly fabricated electrode. Note that 79.8% of the discharge capacity of the material can be retained at a rate of 5.26 Li/h (Figure 3c). Furthermore, performing a signature curve (inset of Figure 3c) did not permanently damage the material as the cell was successfully cycled, afterwards, at a rate of 1 Li in 20 h.

Last, the cycling performance of this compound was tested at 80 °C versus Li in a coin cell with working electrodes consisting of compound **4** (30% by weight), carbon black (20% by weight), and POE (50% by weight). Figure 3d shows the voltage−composition trace of compound **4** cycled at a rate of 1 Li every 20 h at 80 °C. Intercalation voltages, amount of polarization, and capacity per cycle are mostly identical to those determined at room temperature, demonstrating that compound **4** has a great thermal stability, consistent with TGA measurements which reveal no mass variation up to 120 °C. Finally, for the sake of completion, it is also important to note that

(12) Krief, P.; Becker, J.; Ellern, A.; Khodorkovsky, V.; Neilands, O.; Shapiro, L. *Synthesis* **2004**, *15*, 2509–2512.

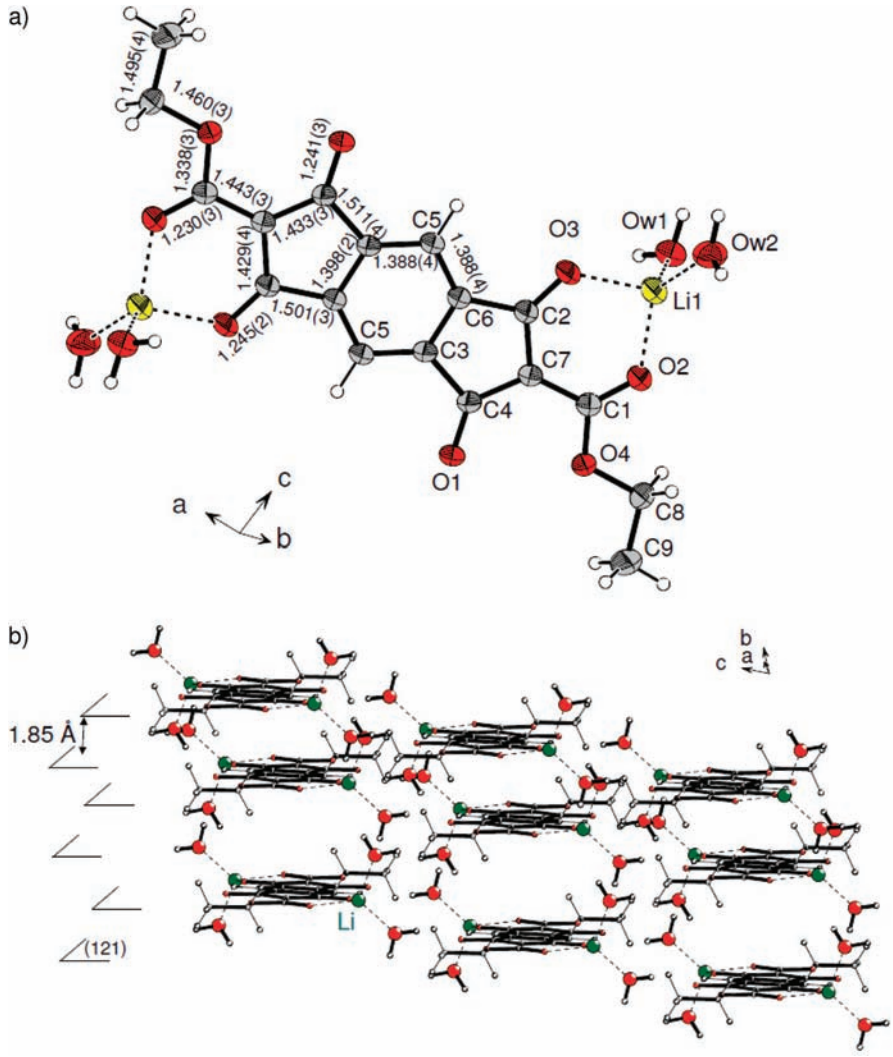

Figure 2. Results of single-crystal analysis: (a) individual $Li_2C_{18}O_8H_{12}\cdot 4H_2O$ group with corresponding label scheme and refined organic distances; (b) macroscopic scale representation of the molecules orienting parallel to the (121) plane, crossing at clusters of water molecules coordinated by lithium in a staggered pattern with an estimated distance between layers of ~1.85 Å.

Table 2. List of Li and H Bond Distances

LiO_4 tetrahedron		water molecules		organic C−H bonds			
Li1−O2	1.932(3)	Ow1−Hw1	0.88(3)	C5−H1	0.98(2)	C9−H4	0.96(2)
Li1−O3	1.965(3)	Ow1−Hw3	0.89(3)	C8−H2	1.010(19)	C9−H5	0.99(2)
Li1−Ow1	1.921(3)	Ow2−Hw2	0.85(3)	C8−H3	1.00(3)	C9−H6	1.04(3)
Li1−Ow2	1.918(4)	Ow2−Hw4	0.84(3)				

crystals of **4** prepared from water as described above and then dehydrated at 120 °C failed to reversibly intercalate Li when cycled in $Li_{2+x}C_{18}H_{12}O_8$/Li cells.

Electrode Analysis: In order to gain further insights into the Li insertion−deinsertion mechanism within this organic compound, we followed the progress of the electrode material by in situ XRD and ex situ proton NMR through one discharge and charge cycle. The electrode material was characterized by in situ XRD while cycling in a specially designed cell.[13] The $Li_{2+x}C_{18}H_{12}O_8$/Li cell was constructed so that the organic electrode material was against a beryllium window; next, the cell was cycled between 1.5 and 3 V at a rate of 1 Li every 20 h while performing XRD measurements once every hour (Figure 4a). For reasons of clarity, we only report the evolution of the XRD patterns in the 10−30° $2\theta_{CuK\alpha}$ range as they reveal most of the relevant action. Upon Li uptake at 1.96 V, a decrease in the main Bragg peaks at $2\theta_{CuK\alpha} = 26$ and 27° is noted as well as the formation of a new doublet near $2\theta_{CuK\alpha} = 27.5$ and 28° corresponding to the growth of a new phase. This change persists until a slight dip in the first plateau at 1.9 V, at which point the newly born phase becomes a unique phase, implying a two-phase insertion process over the $0 < x < 0.5$ Li range in $Li_{2+x}C_{18}H_{12}O_8$ content. Upon further Li insertion, there is again a disappearance of the main peaks at the expense of new ones at $2\theta_{CuK\alpha} = 28$ and 28.5°, which grow and sharpen, indicative of a new phase, as the potential reaches the plateau at 1.67 V. Finally, upon discharging the cell to 1.5 V, a broad Bragg peak

(13) Morcrette, M.; Chabre, Y.; Vaughan, G.; Amatucci, G.; Leriche, J. B.; Patoux, S.; Masquelier, C.; Tarascon, J.-M. *Electrochim. Acta* **2002**, *47*, 3137.

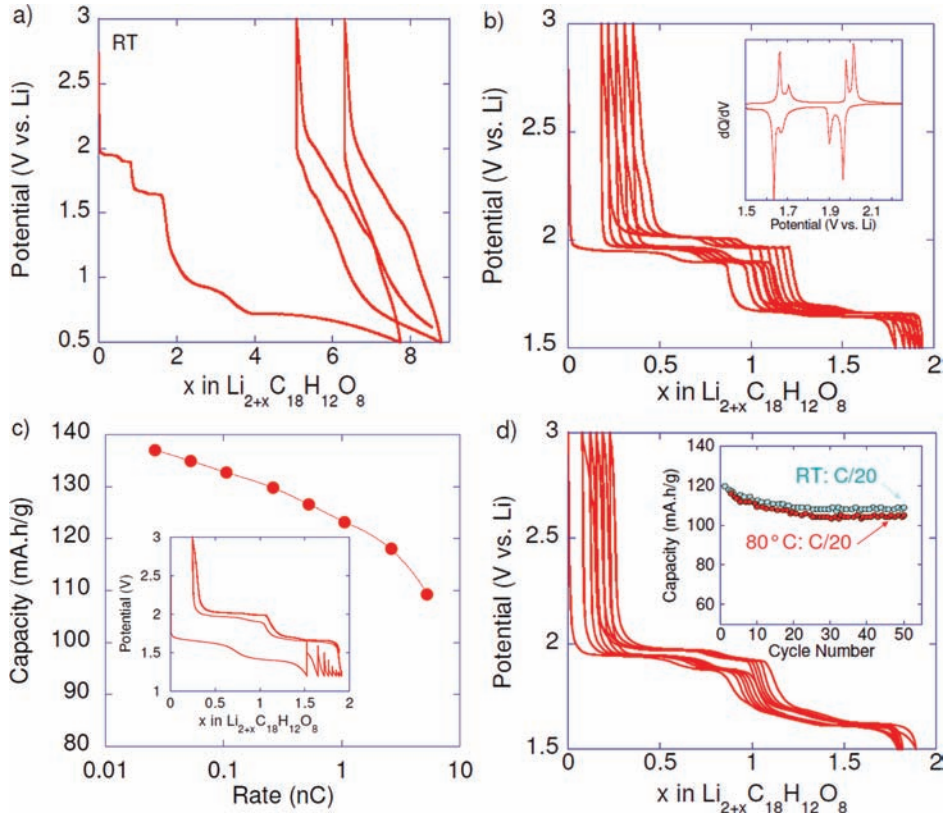

Figure 3. Results of electrochemical analysis on $Li_{2+x}C_{18}H_{12}O_8$/Li cells: (a) potential−composition profile for Swagelok-type cell cycled at a rate of 1 Li^+/20 h between 0.5 and 3 V at room temperature; (b) potential−composition profile for Swagelok-type cell cycled at a rate of 1 Li^+/20 h between 1.5 and 3 V at room temperature, and inset with derivative curve (d*V*/d*Q*); (c) signature curve generated at room temperature, inset with the corresponding potential−composition graph followed by cycling at a rate of 1 Li^+/20 h to demonstrate that the material was not damaged by high rate cycling; (d) potential−composition profile for coin cell cycled at a rate of 1 Li^+/20 h between 1.5 and 3 V at 80 °C, inset with capacity retention curves for cells described in b and d.

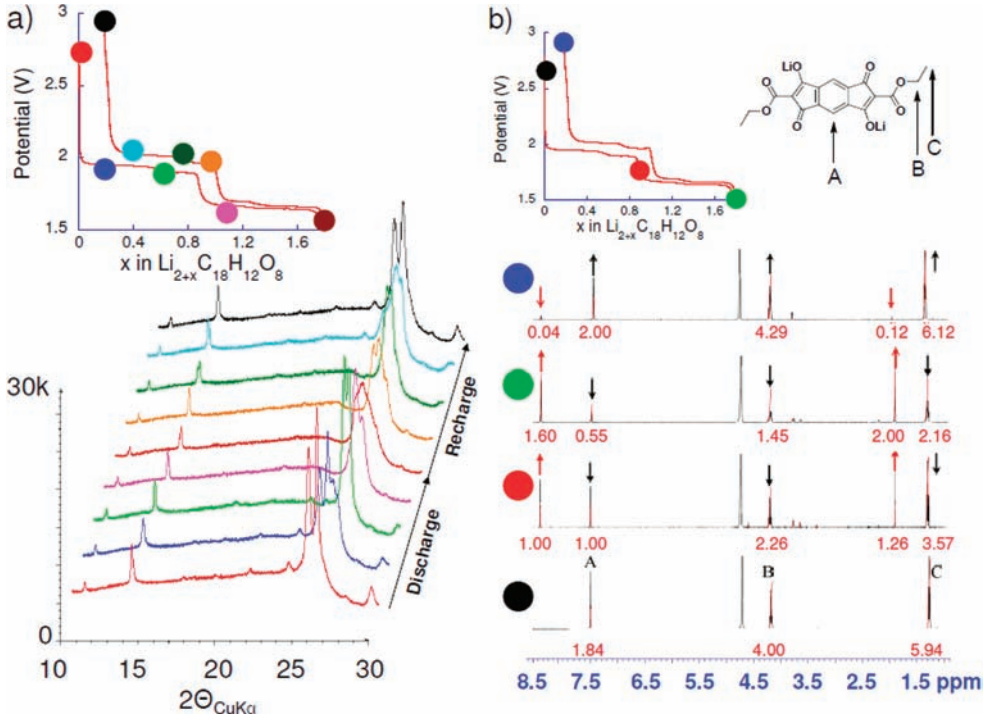

Figure 4. Analysis of electrodes in $Li_{2+x}C_{18}H_{12}O_8$/Li cells cycled at a rate of 1 Li^+/20 h between 1.5 and 3 V at room temperature: (a) in situ XRD measurements, (b) ^{1}H NMR measurements performed in D_2O.

at $2\theta_{CuK\alpha} = 28.5°$ is noted. Once again, as was the case with the first plateau, there is a change in the XRD pattern once the dip in voltage at 1.63 V is reached, signaling that a structural change is affecting the voltage at which Li insertion/deinsertion

occurs. Upon charging the cell, we see the same patterns in reverse until the cell is fully charged; the resulting pattern superimposes on the pattern of the pristine material, indicating a fully reversible process. These numerous structural changes do not come as a surprise bearing in mind the lamellar stacking of this compound. Most likely, they reflect a gliding of the molecules with respect to each other upon Li insertion−deinsertion reactions resulting in two phases differing in energy by a few millielectronvolts, as commonly observed for layered inorganic compounds. At this stage, to prepare larger amounts of partially reduced or fully reduced phases for additional synchrotron studies, it is tempting to use reducing reagents such as *n*-BuLi (as it is common practice in inorganic chemistry). However, *n*-BuLi is an excellent nucleophile capable of reacting with **4**, and therefore, the chemically reduced **4** would most likely have to be prepared via a Birch reduction. Finally, when the cell voltage was lowered below 1.5 V, the XRD pattern did not evolve until $x = 4$, implying carbon reduction within the 1.4−0.7 voltage range, and then became amorphous for greater *x*, suggesting the reductive destruction of the carbonyl groups. Overall, this XRD experiment is significant because it further verifies that the structure of the electrode material, in addition to the electronics of the molecule (e.g., band gap, functional groups to be reduced, etc.), can be utilized in the manipulation of operating voltages and performance of organic electrode materials in batteries.

In order to further demonstrate the reversibility of electrodes composed of compound **4**, ex situ proton NMR studies were performed. The design of the experiment was as follows: three separate Swagelok cells were constructed by grinding compound **4** in a mortar and pestle with 40% carbon black (SP), at which point the cells were cycled at a rate of 1 Li^+ every 20 h with one discharging to 1.8 V, one to 1.5 V, and one fully cycled between 1.5 and 3 V. Next, the electrode material was removed and centrifuged twice with 10 mL of dimethyl carbonate, dried in vacuo at 100 °C for 1 h, followed by the addition of D_2O and filtration of the mixture through a 2 μm syringe filter to remove carbon. Finally, the resulting solution was examined by proton NMR. It is important to note here that, owing to the process of recovering the electrode material and the necessity of using D_2O for solubility reasons, NMR analysis was performed on the hydrolysis product of the material after lithium uptake and not the actual material as it exists within the battery (Figure 4b). Pristine compound **4** displays one aromatic singlet at 7.50 ppm, indicating the cyclopentadieneone groups on each side of the molecule point in opposite directions (anti conformation), and two signals at 4.16 and 1.23 ppm resulting from the CH_2CH_3 of the ester group. When the $Li_{2+x}C_{18}H_{12}O_8$/Li cell is discharged to 1.8 V, the appearance of a second signal in the aromatic region is observed, as well as a decrease by roughly half in the signals associated with the ester group. The appearance of a second aromatic peak indicates that there is a break in the symmetry of the molecule, and this loss of symmetry occurs because when compound **4** (intercalated with one lithium) is exposed to water there is a hydrolysis of one of the ester groups. When the $Li_{2+x}C_{18}H_{12}O_8$/Li cell is discharged to 1.5 V, there is a further decrease in the initial peaks and a further increase in new peaks. This additional reduction in signals associated with the ester groups indicates that the second plateau at 1.67 results from lithium intercalation on the other side of the molecule. The fact that the signals associated with the initial peaks remain after full discharge to 1.5 V results from the molecule not fully intercalating two lithium ions per unit formula. Since evidence provided by proton NMR suggests that the two reductions occur on opposite sides of the molecule (i.e., opposite sides of the aromatic group), the appearance of two major plateaus in voltage−composition traces of $Li_{2+x}C_{18}H_{12}O_8$/Li batteries likely results from either cyclopentadieneone or ester redox centers being held in conjugation with the core of the molecule. The first reduction affects the voltage at which the second reduction occurs through conjugation. This differs from our previous work with dilithium terephthalate,[11] in which two Li-ions are reversibly intercalated at the same voltage. The difference between these two systems arises from the orientation of the active groups to be reduced with the conjugated backbone of the molecule. In the case of dilithium terephthalate, the most probable orientation of the carbonyl functionalities is perpendicular to the phenyl core, due to steric interactions; as a result, each carbonyl can be reduced at the same voltage because it is not in conjugation and is consequently minimally affected by reduction of the other carbonyl group. Finally, when the cell undergoes one full cycle between 1.5 and 3 V, the resulting NMR spectrum is consistent with the pristine material, thus indicating a fully reversible process. Now a question dealing with the voltage sequence reduction of the ester and cyclopentadieneone functionalities remains. Proton NMR seems to suggest that reduction of the molecule between 3 and 1.5 V occurs at the ester groups because of the observed hydrolysis of the ester group upon treatment of reduced compound **4** with water; however, when the same procedure as described for ex situ NMR was repeated for IR studies (Supporting Information S3 and S4), C═O stretches for both the ester and the cyclopentadieneone decreased upon discharge of the battery. Therefore, further studies are required to definitively determine where reduction of the molecule occurs.

Conclusions

We have reported a new organic molecule containing both carbonyls and ester redox centers capable of reversibly reacting with two lithium ions leading to a sustained capacity of 110 mAh/g for at least 50 cycles. The insertion process occurs via a stair case voltage decay with plateaus at 1.9 and 1.5 V. The lower irreversible plateau a 0.7 V corresponding partially to the reduction of C═O groups is somewhat unexpected and intriguing. DFT calculations are presently being carried out to test the theoretical underpinning of this observation. The voltage anomalies in the charge−discharge curves were shown, via XRD studies, to be linked to rearrangements of the 3D stacking of the molecules. High-resolution synchrotron experiments remain to be done to clarify this point. Finally, this work illustrates the richness of organic chemistry in producing organic electrodes capable of reversibly reacting with Li, enlisting the ester function as the redox center. Efforts to tune the redox voltage through chemical modification of the aromatic core of the molecule are presently under consideration.

Experimental Section

General: Chemicals were purchased from Sigma-Aldrich Chemical and Fisher Scientific and used without further purification unless stated otherwise. Solvents, where applicable, were distilled from Na/benzophenone, CaH_2, or K_2CO_3. NMR spectra were obtained on a Bruker DMX 500 MHz spectrometer utilizing Topspin software.

Synthesis: Lithium 2,6-bis(ethoxycarbonyl)-3,7-dioxo-3,7-dihydro-*s*-indacene-1,5-bis(olate) (4). To a stirred solution of compound **3** (0.250 g, 0.698 mmol) in 100 mL of methanol was added LiOH (0.060 g, 1.43 mmol), and the reaction was capped

and allowed to proceed overnight at room temperature. The red suspension was then collected through centrifugation and dried in a vacuum oven at 60 °C (0.2356 g, 91.24%): ^{1}H NMR (D_2O) δ 1.20 (6H, t), 4.12 (4H, m), 7.40 ppm (2H, s); ^{13}C NMR (D_2O) δ 13.90, 59.59, 94.30, 98.52, 111.77, 142.25, 166.51, 192.69, 202.50 ppm.

Single Crystal: The single-crystal structure of **4** was obtained with a Bruker X8 four axes diffractometer with Mo Kα X-ray source. Tables S1 and S2 contain supplementary crystallographic data for this paper. This data can be obtained free of charge from The Cambridge Crystallographic Data Centre via www.ccdc.cam.ac.uk/data_request/cif.

Powder Diffraction: X-ray powder diffraction patterns were collected on a Bruker D8 diffractometer utilizing Cu Kα radiation, equipped with a Gobel mirror and a Braun PSD detector and operating at 40 kV, 30 mA in the range $2\theta_{CuK\alpha} = 10-100°$ with a 2θ step size of 0.017°.

Electrochemical Studies: Two types of cells were constructed.

Swagelok cells were constructed utilizing a disk of Li metal as the negative electrode and a Whatman GF/D borosilicate glass fiber sheet saturated with an electrolyte consisting of 1 M $LiPF_6$ in a 1:1 (w/w) mixture of ethylene carbonate/dimethyl carbonate solution. Working electrodes were constructed by mixing in a mortar and pestle compound **4** with 40% (by weight) carbon black (SP). For Swagelok batteries, 10−13 mg of the mixture was utilized. The signature curve was obtained using an electrode loaded with 5 mg of active material per cm^2.

PEO-based coin cells for cycling at 80 °C were constructed utilizing a disk of Li metal as the negative electrode and a polymer electrolyte film consisting of a 20:1 molar ratio of PEO (9:1 ratio by weight of 100 000M_w/4 000 000M_w) to $LiClO_4$ as the separator. Working electrodes were constructed by mixing in a mortar and pestle compound **4** (30% by weight), carbon black (20% by weight), and POE (50% by weight) followed by the addition of a minimal amount of acetonitrile. This paste was then applied to the coin cell in such a way as to end up with 5−6 mg of the mixture following evaporation of the solvent.

All electrode mixing and battery construction was performed in an argon-filled glovebox. Galvanostatic charge−discharge experiments were conducted at 20 °C using a VMP system (Biologic S.A., Claix, France) operating in galvanostatic mode. Unless otherwise stated, the cells were cycled between 1.5 and 3 V versus Li^+/Li^0 at one Li^+ exchanged per 20 h.

Acknowledgment. We would like to thank M. Armand and P. Poizot for enlightened scientific discussions.

Supporting Information Available: Atomic coordinates and isotropic thermal displacement parameters, as well as anisotropic thermal displacement parameters from single-crystal measurements, and the results of ex situ IR studies for $Li_{2+x}C_{18}H_{12}O_8$/Li cells cycled at a rate of 1 Li per 20 h between 1.5 and 3 V. This material is available free of charge via the Internet at http://pubs.acs.org.

JA1012849